Numerical experiments on Yang-Lee zeros

1986 J. Phys. A: Math. Gen. 19 2611

(http://iopscience.iop.org/0305-4470/19/13/026)

J. Phys. A: Math. Gen. 19 (1986) 2611-2624. Printed in Great Britain

Numerical experiments on Yang–Lee zeros

D W Wood and R W Turnbull

Department of Mathematics, University of Nottingham, Nottingham NG7 2RD, UK

Received 2 December 1985

Abstract. It is argued that since any real space renormalisation R is a transformation under which the partition function is invariant, those R which are based upon various real space approximation schemes can in principle be extended into the complex field of the parameter space. In this extension the Julia set of R (now extended to include R which are algebraic) is an approximation to the locus of the Yang-Lee zeros. Finite-size scaling using Onsager's solution of the two-dimensional Ising model is used to construct R which are highly accurate in real temperatures in the critical region; these are extended into the complex temperature plane and results are displayed for both the anisotropic and isotropic cases.

1. Introduction

To obtain the limiting distribution of the partition function zeros (Yang and Lee 1952a, b) in the complex temperature plane for model problems in statistical mechanics is well known to be a difficult problem. Very few exact results are known (Fisher 1965, Bruscamp and Kunz 1974, Wood 1985a) and there has been a renewed interest in approximate methods to locate the locus of the Yang-Lee zeros. Until recently the location of a discrete set of zeros of the partition functions of small finite lattice sections seems to have been the only computational method adopted (examples are Pearson 1982, Martin 1983, Ono *et al* 1967, 1968). The nature of this problem for hierarchical lattices is, however, very much simpler since the Yang-Lee zeros are simply the Julia sets of rational complex maps which are known exactly. For such lattice types the Yang-Lee zeros can be computed on a sequence of inverse iteration of a particular rational map, which is the renormalisation transformation of a given model (Derrida *et al* 1983, Itzykson and Luck 1983).

An interesting attempt to extend a 'real' space renormalisation method into the complex temperature plane has recently been proposed by Derrida and Flyvbjerg (1985) and applied to the two-dimensional Ising model. These authors introduce a renormalisation transformation R based upon a finite-size scaling argument using three finite lattices; R is viewed as a 'good' approximation to a 'true' R and again the Julia set of this transformation is computed. A proposal for a different mathematical approach to the problem has recently been outlined by one of us (Wood 1985b), in which the whole *limiting distribution* for at least a semi-infinite system can be found using the eigenvalues of finite transfer matrices; the details of this approach will be the subject of a further publication.

The purpose of the present publication is to present the results of some numerical experiments on the Yang-Lee zeros of the two-dimensional Ising model. In one part we adopt a similar viewpoint to that of Derrida and Flyvbjerg (1985) in the extension

0305-4470/86/132611+14$02.50

of real space renormalisation transformations into the complex field; for the other part we adopt a naive approach which does not involve a renormalisation transformation and uses only one semi-infinite lattice system. Within each of these schemes results are displayed for both the isotropic and anisotropic models.

2. Fixed point sets and large rescaling

In the case of a hierarchical lattice (Derrida *et al* 1983) of n 'steps', real space renormalisation can be given an exact representation whereby, if $Z_n(z)$ is the partition function of some given one-parameter model Hamiltonian and z is any convenient temperature variable, then a recursive sequence of the form

$$Z_n(z) = G(z)Z_{n-1}(z') \tag{1}$$

can in principle be constructed exactly. Here $G(z)$ is a simple analytic factor and z' is the renormalised temperature variable obtained under a known renormalisation transformation

$$z' = R(z). \tag{2}$$

Thus the zeros of Z_n are the pre-images of the set of zeros of Z_{n-1} under R. In this way Derrida *et al* (1983) have computed the Julia sets of (2) for examples of the scalar q-state Potts models where R is typically a simple rational map. Although the fact that for hierarchical lattices (2) is an exact renormalisation is an enabling feature of the work of Derrida *et al*, the fundamental property of a real space renormalisation R in an application to the Yang-Lee zeros is the property that a true renormalisation must keep the partition function invariant, namely

$$Z_n(\mathcal{H}) = Z_{n'}(\mathcal{H}') \qquad (n' < n) \tag{3a}$$

$$z' = R(z) \tag{3b}$$

where $(\mathcal{H}')$ is the renormalised reduced Hamiltonian. Thus the Yang-Lee zeros will be the Julia sets of R which are now extended to included maps which are not rational. A simple example of this on a non-hierarchical lattice is the one-dimensional Ising model in a magnetic field; following Nelson and Fisher (1975) the model has a two-variable parameter space $x = e^{-4K}$, $y = e^{-2L}$ ($K = J/kT$, $L = H/kT$) in which (3b) is given exactly by

$$x' = x(1+y)^2/(x+y)(1+xy) \tag{4a}$$

$$y' = y(x+y)/(1+xy). \tag{4b}$$

If we extend (4a) and (4b) into the complex y plane, in which the Yang-Lee zeros lie on the unit circle (Yang and Lee 1952b), we readily verify that these equations restrict y' to move on this circle and x' to be real. Thus if $y = e^{i\phi}$ and x real:

$$y' = e^{2i\psi} \qquad \left(\tan\psi = \frac{\sin\phi}{x+\cos\phi}\right) \tag{5a}$$

$$x' = \frac{4x\cos^2\frac{1}{2}\phi}{x^2+2x\cos\phi+1}. \tag{5b}$$

In a recent letter Derrida and Flyvbjerg (1985) have proposed the construction of an approximate R using the partition functions of three finite lattices and argue that since these are all polynomials in form the real axis plays no preferred role. Thus an extension of $(3b)$ into the complex field is acceptable. While we indeed agree with this argument there seems to the present authors absolutely no reason why it should be restricted to approximations to R in which $(3b)$ becomes implicit and composed only of rational functions (the map itself will of course not be rational). Indeed for any one of the many ways in which approximations to $(3a)$ and $(3b)$ can be formed (for a review see Burkhardt and van Leeuven 1982), the approximation represents an attempt to find an approximation to R, R_α say, under which Z_n is invariant. Hence R_α is by construction an approximation to an 'object' which maps zeros into zeros and thus it seems quite proper to view the extended Julia set of R_α as the approximation to the Yang-Lee zeros within the particular approximation scheme of R_α.

Renormalisation transformations R which are not simple rational maps but are expressed implicitly in terms of either rational or algebraic functions will typically present quite formidable computational problems in constructing sequences of inverse iterates and the Julia set will be extremely difficult to obtain. If, however, we consider an exact R with, say, a large rescaling factor b we can view this as physically equivalent to a sequence of m successive applications of a renormalisation R' with a smaller rescaling factor b' where

$$R = (R')^{(m)} \qquad b^{1/m} = b' \tag{6}$$

and correspondingly for an approximation scheme

$$R_\alpha \simeq (R'_\alpha)^{(m)}. \tag{7}$$

Thus if z_0 is one fixed point of R, the periodic cycle sequence

$$(R')^{(j)}(z_0) = \{z_1, \ldots, z_j\} \qquad (1 \leqslant j \leqslant m) \tag{8}$$

is a fixed point set of R. Now if we consider $(3a)$ for a large rescaling factor $(n' \ll n)$ we expect $(3b)$ to possess a large number of fixed points; the cycle points may be contained in both the Julia sets of R and R'. This is simply the observation that for an increasingly large rescaling $(3a)$ requires that each zero of the reduced system corresponds to an increasingly large number of zeros in the original system. The implication here is that for $n' \ll n$, where the Yang-Lee zeros lie on a simple curve, say, the fixed points of R above may provide a good enough view of the limiting distribution as a whole. The zero-field one-dimensional Ising model offers a trivial example of this, where for $b' = 2$ $(3b)$ is simply

$$v' = v^2 \qquad (v = \tanh K) \tag{9}$$

but for a rescaling of $b = 2^m$

$$v' = v^{2m} \tag{10}$$

which in its fixed points locates $2m - 1$ points on the limiting locus $|v| = 1$.

Our proposition in the first instance therefore is that the fixed points of R with a large b in the complex field will probably be clustered close to the limiting distribution, and of course these are easy to find compared with trying to construct the whole Julia set. However, constructing an R_α $(\simeq R)$ with a large rescaling factor is of course a very difficult thing to do, and to test these ideas we have used the finite-size scaling scheme of Nightingale (1982) (for a review see Barber 1983) in conjunction with the exact

solution of Onsager (1944) for the two-dimensional Ising model for *both* the isotropic and anisotropic cases. Here the finite-size scaling transformation generates R_α in terms of the correlation lengths (real variables) of two semi-infinite strips of the quadratic lattice. Thus if the two strips have widths n and m and $\lambda_1(n, z)$ and $\lambda_2(n, z)$ are the two eigenvalues of the transfer matrix which are greatest in modulus (z real), then R_α is given by

$$|\delta'|^n = |\delta|^m \qquad (b = m/n) \tag{11}$$

where

$$\delta' = \frac{\lambda_2(z', n)}{\lambda_1(z', n)} \qquad \delta = \frac{\lambda_2(z, m)}{\lambda_1(z, m)}. \tag{12}$$

The eigenvalues $\lambda_1(z, n)$ and $\lambda_2(z, n)$ are given by

$$\lambda_1 = (2z)^{n/2} \prod_{i=1}^{n} \exp(\tfrac{1}{2}\gamma_{2i-1}) \qquad \lambda_2 = (2z)^{n/2} \prod_{i=1}^{n} \exp(\tfrac{1}{2}\gamma_{2i}) \tag{13}$$

where

$$\cosh \gamma_j = z + z^{-1} - \cos j\frac{\pi}{n} \qquad z = \sinh 2K \qquad \text{(isotropic case)}. \tag{14}$$

Our proposal is to formally extend (11) into the complex field, *but* to regard (11) as a map from z to z' and to attempt inverse iteration would be both a formidable and dangerous undertaking, so following the above discussion we have in the first instance taken $n\,m$ sequences for large rescaling factors b and computed a sample of the fixed points of (11) in the $\sinh 2K$ plane where the Yang–Lee distribution is on the unit circle (Wood 1985a). The danger alluded to above refers to the care needed in identifying the appropriate branches of the functions e^{γ_j}, each of which is an algebraic function of $\cosh \gamma_j$ with two branches. The results of these calculations are shown in figures 1 and 2 for $b = 30$ and 40. These pictures, however, are only a small projection of the overall view (shown below) obtained from (11). They merely show that a small but systematic sampling of the transformations yield fixed point sets which are indeed clustered and very close to the exact locus. The fixed points shown in figures 1 and 2 are joined with line segments only to highlight their distribution relative to the unit circle.

Insofar as the Ising model is a suitable testing ground the outcome of the calculations in figures 1 and 2 is very satisfactory. The points in these figures are obtained with R_α in the form (11), but a full extension to the complex field should really replace (11) by the form

$$(\delta')^n = \delta^m. \tag{15}$$

The use of the modulus sign in (11) originates from identifying the finite-size scaling transformation physically as a rescaling of the correlation range in the critical point region. In fact, even for z real, λ_2 can be complex (or real negative), and it *will* probably be so if the low temperature phase or ground state is translationally symmetric with respect to a unit cell of the lattice any larger than a single site. Thus, to include the antiferromagnetic region (real variables) for the Ising model case here (where λ_2 would be negative), the full extension to the complex field (15) is required. Again

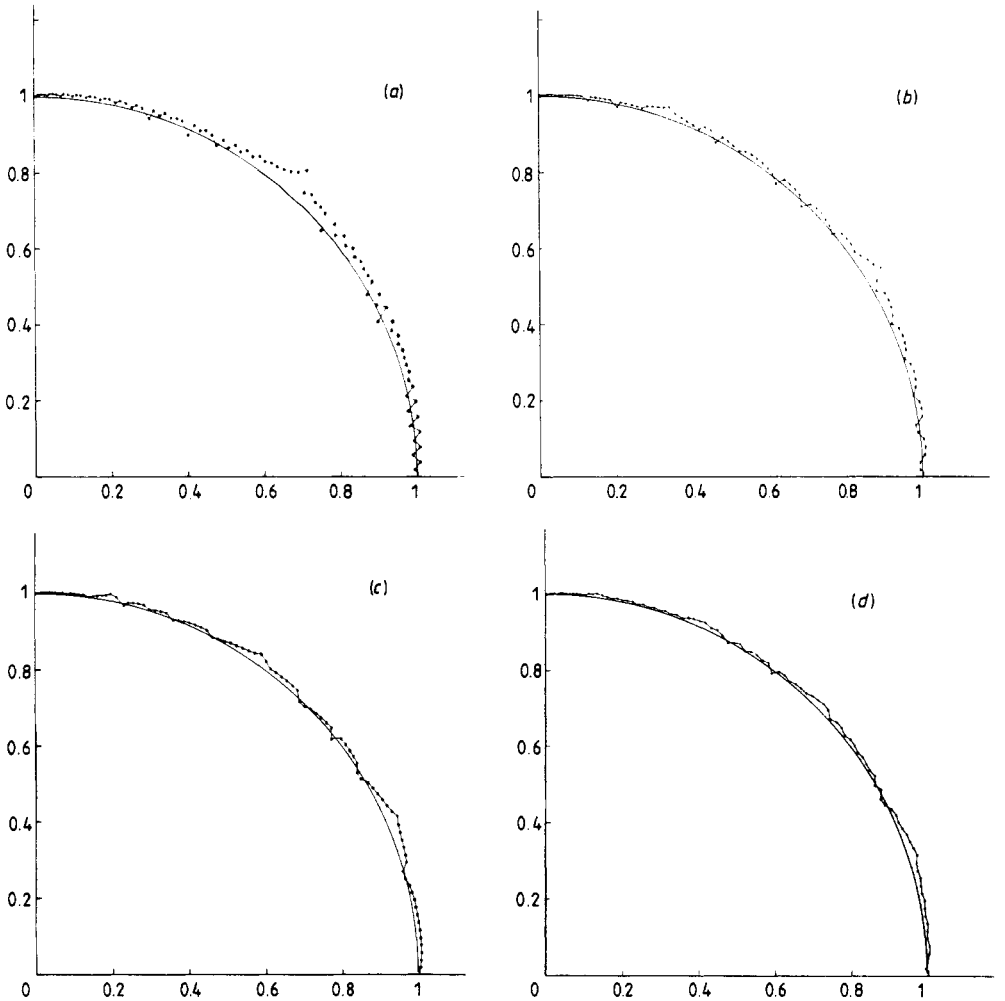

Figure 1. Samples of the fixed points of equation (11) in the sinh $2K$ plane for sequences n, m in which $b = 30$; the exact locus is the circular arc $|s| = 1$. $(m, n) = (a)$ 60, 2; (b) 90, 3; (c) 120, 4; (d) 150, 5.

using a fairly large rescaling factor of 10 and 20 and now looking with a much higher resolution at the two equations (11) and

$$n \arg \delta' = m \arg \delta \tag{16}$$

we find that the two fixed point sets of (11) and (16) are indeed highly concentrated close to the exact locus. The two examples are shown in figures 3 and 4 but now in terms of the variable $z = e^{-2K}$ where the distribution on the two circles is

$$z = \pm 1 + \sqrt{2}\, e^{i\phi} \qquad (0 \leqslant \phi \leqslant 2\pi) \tag{17}$$

shown by the continuous line (Fisher 1965, Wood 1985a). The true fixed point set to (15) is of course the intersection of the two fixed point sets of (11) and (16), but this is too awkward to display separately. As it is, each one of (11) and (16) is tied down very closely to the final distribution. The tracings of the graph plotting algorithm

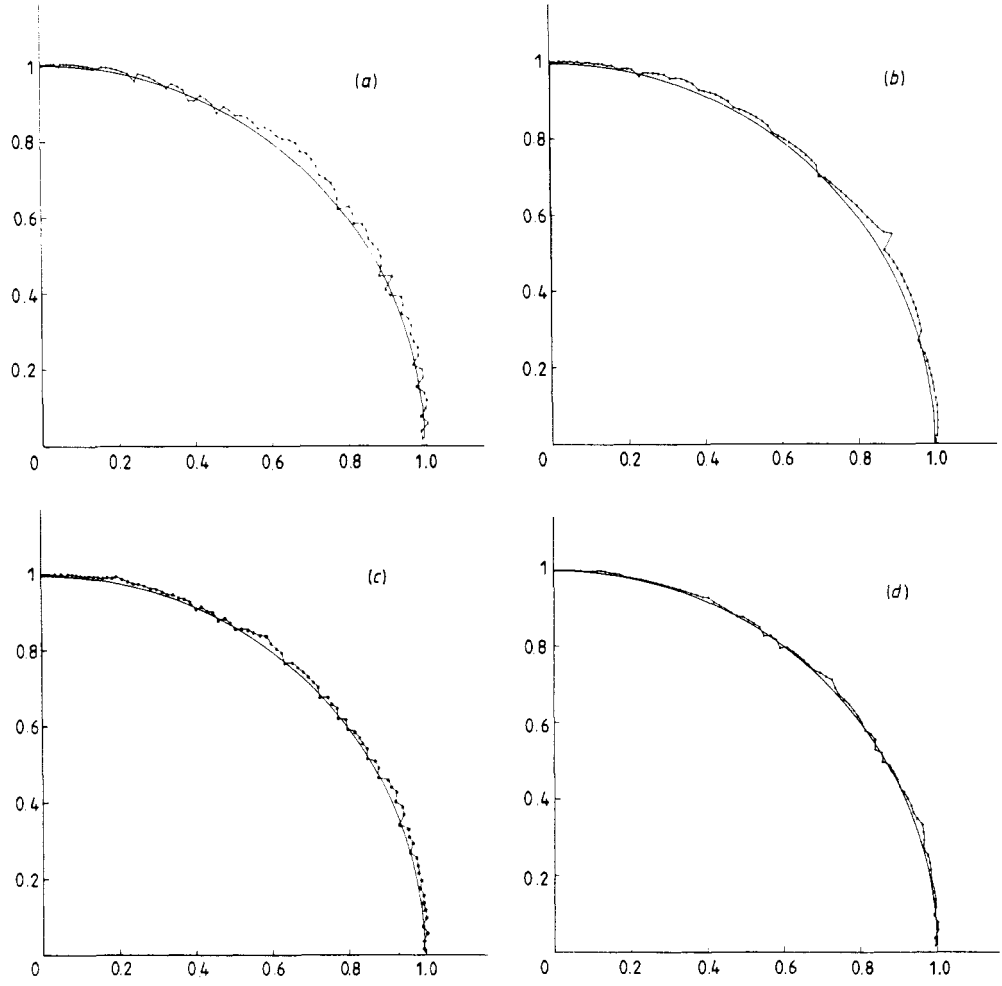

Figure 2. Samples of the fixed points of equation (11) in the sinh $2K$ plane in which $b = 40$; the exact locus is the circular arc $|s| = 1$. $(m, n) = (a)$ 80, 2; (b) 120, 3; (c) 160, 4; (d) 200, 5.

inside the two circles (17) which appear in figures 3(b) and 4(b) and again below in figures 7(b) and 8(b) are probably spurious.

3. Small rescaling lengths

The finite-size scaling transformation (11) has been remarkably successful both in its application to critical point behaviour (for a review see Barber 1983) and in the study of phase equilibrium generally (Wood and Osbaldestin (1983), Osbaldestin *et al* 1985). Equation (11) restriced to real temperatures, typically with $m = n + k$, (k small), has produced many remarkable numerical estimates of critical parameters (see, for example, Wood and Goldfinch 1980, Baxter *et al* 1980). Encouraged by the previous results we have considered the extension (15) of (11) for cases where $m = n + 1$. An extension of this type has some similarities to moving from a one-parameter space to a

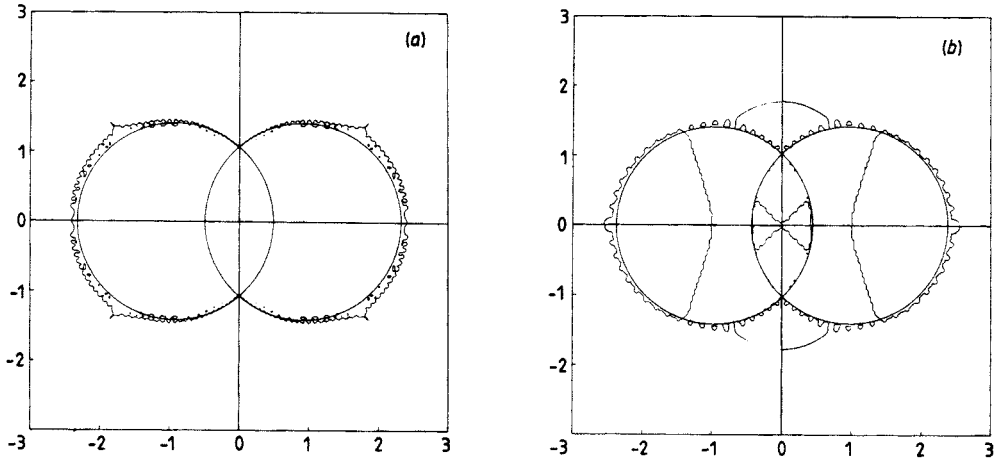

Figure 3. (*a*) The fixed point sets of (11) and (*b*) of (16) shown for $b = 20$ ($m = 40$, $n = 2$), with a high resolution for the isotropic Ising model in the complex plane of $z = \exp(-2K)$. The exact locus is the intersecting circles shown by the continuous line.

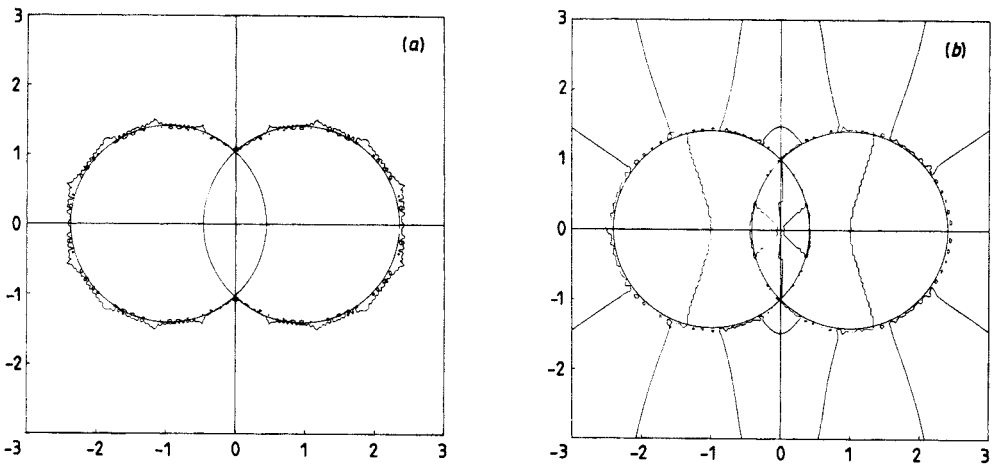

Figure 4. (*a*) The fixed point sets of (11) and (*b*) of (16) shown for $b = 10$ ($m = 50$, $n = 5$), with a high resolution for the isotropic Ising model in the complex plane of $z = \exp(-2K)$. The exact locus is the intersecting circles shown by the continuous line.

two-parameter space and it is useful to consider again the nature of (11) for real variables as it applies to the ferromagnetic and isotropic Ising model. At the critical temperature and for all temperatures below it, the two eigenvalues are identically equal in the thermodynamic limit $n \to \infty$. Such limiting behaviour is closely approximated by (11) for finite n and m (as illustrated by Wood and Osbaldestin 1982) and is shown in figure 5. On including the magnetic field into (11) that portion of the curve in figure 5 above the axis is still very tightly constrained in the *real* field-temperature plane, and is illustrated in figure 6 where the hairpin zero contour is the approximation to the coexistence curve $0 \leqslant T \leqslant T_c$, $H = 0$.

The relevance of this feature in the complex field is substantial in that we anticipate, for a sequence of R_α which are very faithful to the original Hamiltonian, the fixed points (11) and (16) could become asymptotically dense in what is the complex analogue

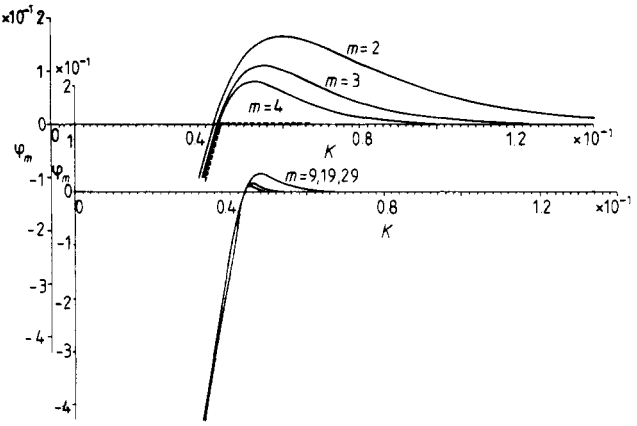

Figure 5. Plots of the function $\phi_m = m \ln|\delta'| - (m+1)\ln|\delta|$ (see (11)) against the variable $K = J/kT$ for $m = 2, 3, 4, 9, 19$ and 29 in the case of the isotropic Ising model (from Wood and Osbaldestin 1982).

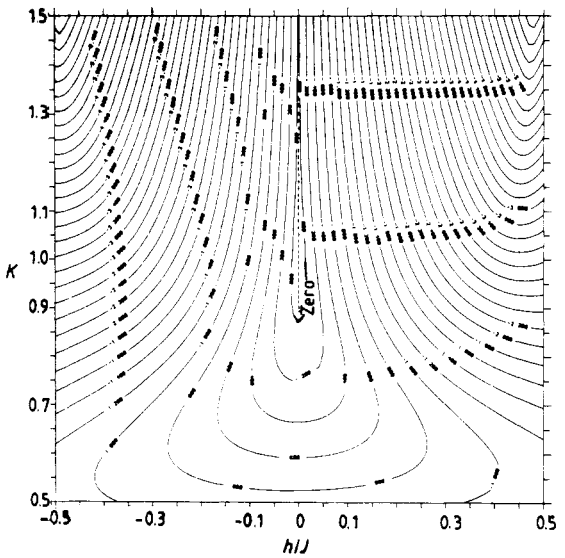

Figure 6. Contour plots of the function $n \ln|\delta'| - (n+1)\ln|\delta|$ (see (11)) in the real temperature ($K = J/kT$) field (H/J) plane for the isotropic Ising model with $n = 4$; the broken line is the coexistence curve (from Wood and Osbaldestin 1982).

of the low temperature region. For the Ising model γ_0 in (14) plays the crucial role of producing a transition in the thermodynamic limit, and in fact for the isotropic model the locus of Yang-Lee zeros is simply traced out by the contour $\gamma_0 = i\phi$ in the complex plane (Wood 1985a) and in the general anisotropic case (horizontal : vertical interactions = $K : K'$)

$$\gamma_0 = 2K^* - 2K' = i\phi \qquad \exp(-2K^*) = \tanh K \qquad 0 \leqslant \phi \leqslant 2\pi \quad (18)$$

traces out the boundaries of the limiting distribution. For large n where $\gamma_1 \sim \gamma_0$ or $\gamma_1 \sim -\gamma_0$ across the boundary in (18), the complex 'low' temperature domain is the region where $\gamma_1 \sim \gamma_0$ and in this domain λ_1 and λ_2 of (13) are identically equal in the

thermodynamic limit. In this domain we expect that the zeros of the two functions

$$\Delta_1 = |\delta'|^n - |\delta|^m \tag{19a}$$

and

$$\Delta_2 = n \arg \delta' - m \arg \delta \tag{19b}$$

will have characteristics illustrating this effect as n and m increase. With $m = n+1$ and in the limit $n \to \infty$, the Yang-Lee zeros would be the boundaries of domains where the fixed points are dense.

The zero contours of Δ_1 and Δ_2 in the complex $z = e^{-2K}$ plane are shown for $n = 20$ and 30 in figures 7 and 8, where the system of spokes emerging from the rim of the

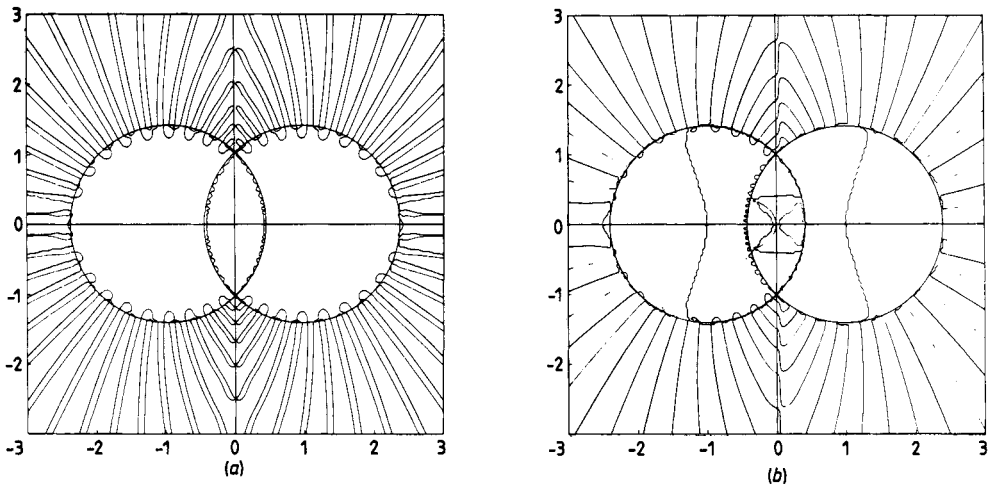

Figure 7. (*a*) The fixed point set of (11) and (*b*) of (16) for $m = n+1$, $n = 20$ in the $z = \exp(-2K)$ plane. The system of spokes resprsents the onset of a dense region bordering the locus of Yang-Lee zeros.

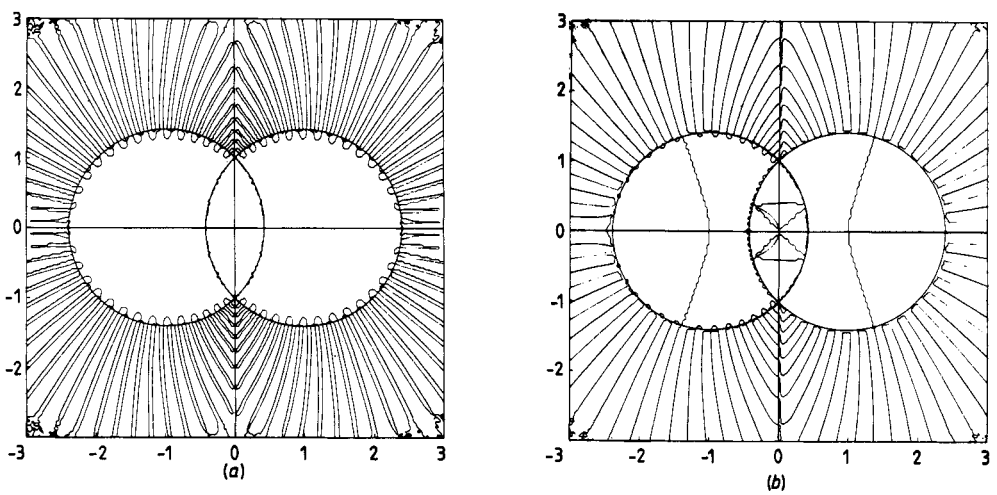

Figure 8. (*a*) The fixed point set of (11) and (*b*) of (16) for $m = n+1$, $n = 30$ in the $z = \exp(-2K)$ plane. The system of spokes represent the onset of a dense region bordering the locus of Yang-Lee zeros.

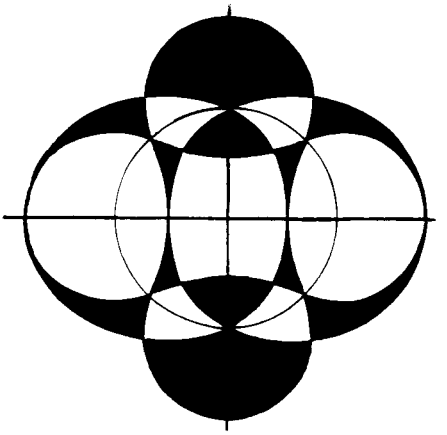

Figure 9. The Yang-Lee distribution (shown shaded), for the anisotropic Ising model with K: $K' = 1:2$ in the complex plane of $z = \exp(-2K)$ (from Wood 1985a).

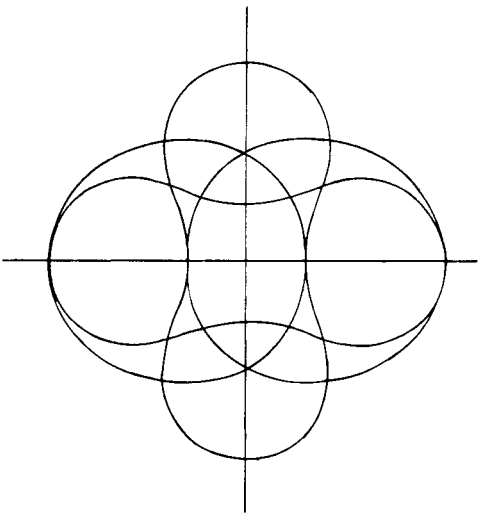

Figure 10. The boundary curves of the Yang-Lee distribution with K: $K' = 1:2$ in (18) in the complex plane of $z = \exp(-2K)$ (from Wood 1985a).

two intersecting circles (note that here the intersection has emerged very clearly (cf figures 1 and 2)) represent the onset of a dense set obtained in the limit $n \to \infty$.

We have also included the anisotropic case of the two-dimensional Ising model in these calculations. Here (18) traces out the boundaries of the Yang-Lee distribution for a general parametrisation K: K'; and in the case where $K : K' = 1:2$ the Yang-Lee zeros fall in the shaded regions of figure 9 which have the four boundary curves shown in figure 10. The scaling transformation calculations for $n = 10$ and 20 of (11) are

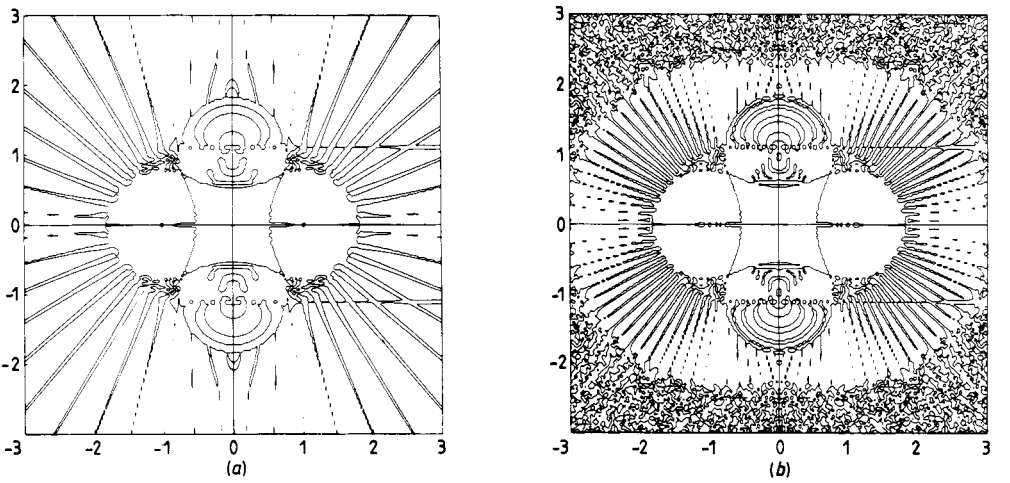

Figure 11. The same as figure 7(*a*) for the anisotropic Ising model with $K : K' = 1:2$ and $n = 10$ and 20 where (11) has been adapted to produce *only* the dumb-bells in figure 10. (*a*) for $n = 10$ and (*b*) for $n = 20$.

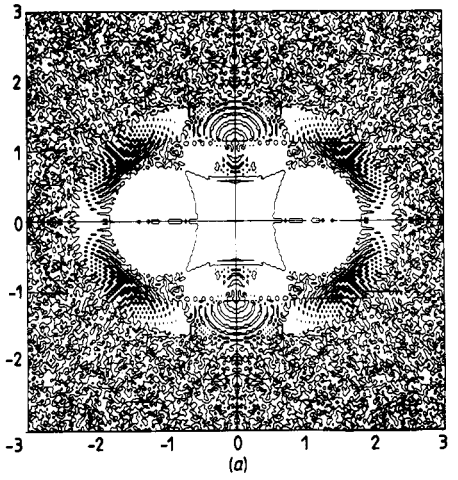

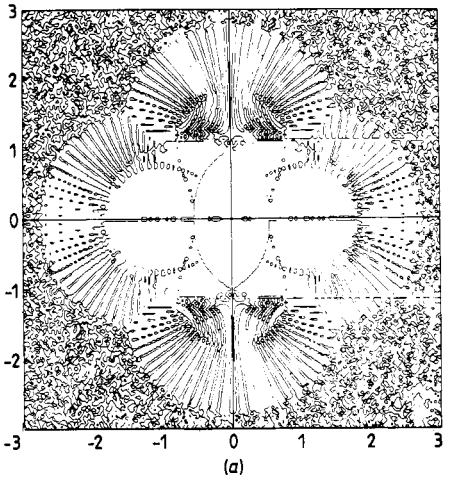

Figure 12. (a) and (b) are respectively the fixed point sets of (11) for the anisotropic Ising model with $K:K'=1:2$ and $K:K'=2:1$, $n=40$, in the plane of $z=\exp(-2K)$.

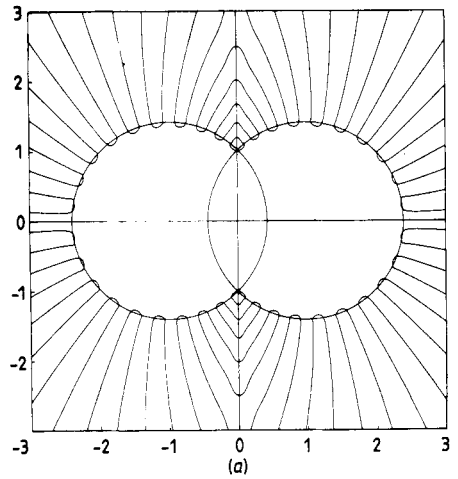

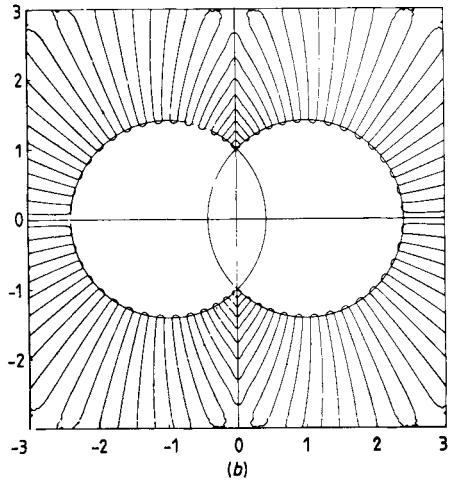

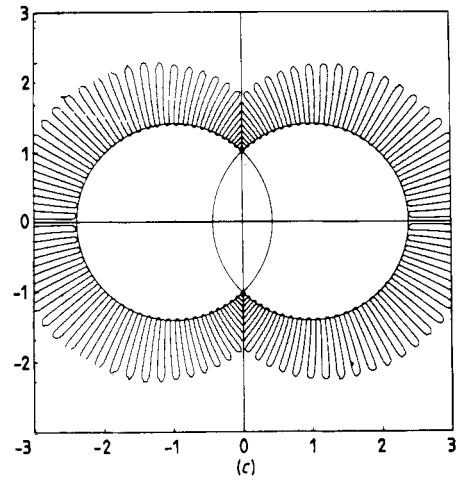

Figure 13. The loci generated by (21) using single systems with (a) $n=20$, (b) $n=30$ and (c) $n=50$.

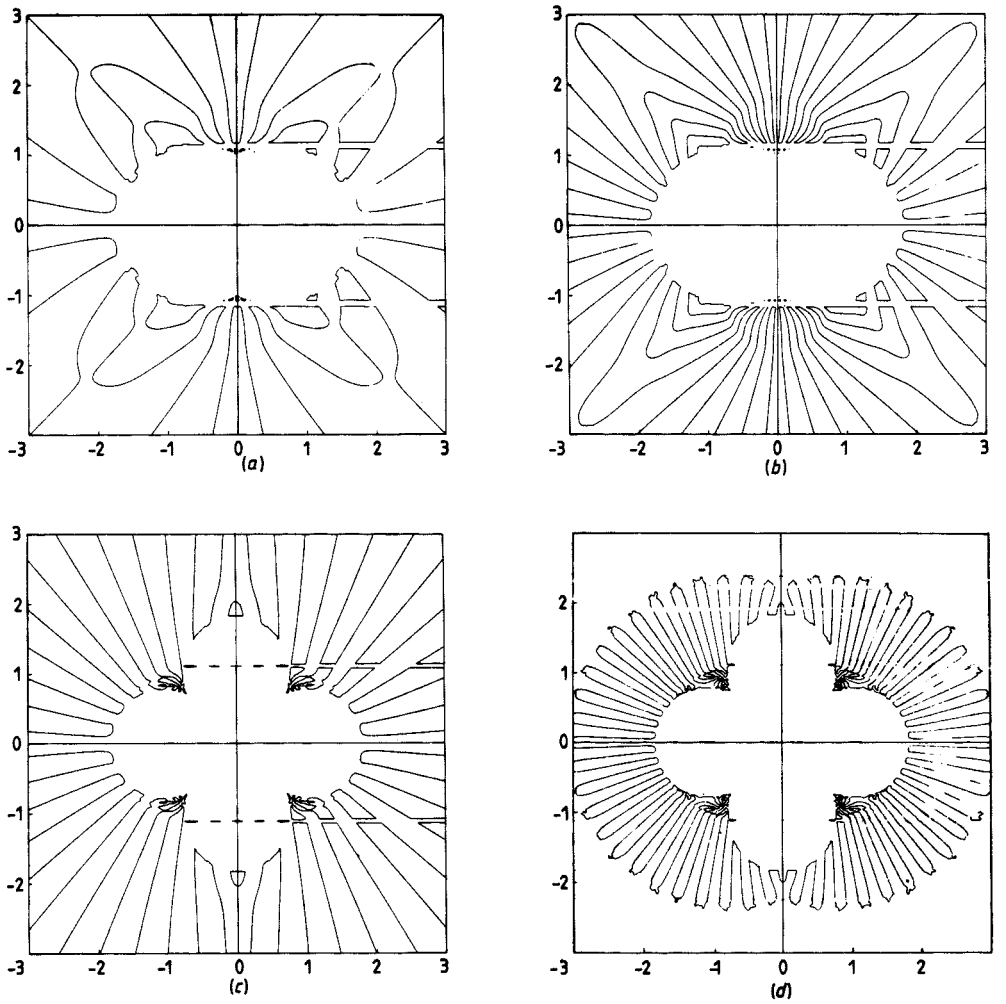

Figure 14. The loci of (21) for the anisotropic model $K:K'=1:2$; (*a*) $n=10$ and (*b*) $n=20$ for the loci which approximate the two squashed circles in the boundaries shown in figure 10, and (*c*) $n=10$ and (*d*) $n=20$, which approximate the dumb-bell boundary curves shown in figure 10.

shown in figure 11 and for $n=40$ in figure 12. The system of two interacting dumb-bells is clearly discernable in figure 11, where in these calculations we have used (11) in a way which should only pick out the two dumb-bells in figure 10 ($K:K'=1:2$) and *not* the two 'squashed' circles ($K:K'=2:1$) (see Wood 1985a). In figure 12(*a*), (11) has been used to pick out the dumb-bells and figure 12(*b*) the two squashed circles.

4. Approximations using a single lattice system

A naive approach to the Yang-Lee zeros is possible using only a single lattice system, whereas any technique using a renormalisation transformation R clearly requires at least two lattices. In the isotropic Ising model the locus of zeros is given by (18) which

is equivalently expressed in the form

$$\lim_{n\to\infty} \frac{\lambda_2(n, K)}{\lambda_1(n, K)} = e^{-\gamma_0} = e^{i\phi} \qquad 0 \leqslant \phi \leqslant 2\pi. \tag{20}$$

Hence a sequence on n of loci generated by

$$|\lambda_2(n, K)/\lambda_1(n, K)| = 1 \tag{21}$$

should converge onto the limiting distribution which again should appear as the boundary of a dense set. The orbits traced out by (21) with $n = 20$, 30 and 50 are shown in figure 13 and corresponding orbits for the anisotropic model with $K : K' = 1 : 2$ are shown for $n = 10$ and 20 in figure 14. Here, both the boundaries generated by $K : K' = 1 : 2$ (the dumb-bells) and $K' : K = 1 : 2$ (the squashed circles, see Wood 1985a) are shown. The absence of those portions of the two circles (17) *inside* the boundaries approximated in figure 13 is merely an artefact produced by our selection of the branches of the two functions e^{γ_0} and e^{γ_n} of (14) in performing the numerical calculations. In the cosh γ_0 and cosh γ_n planes both e^{γ_0} and e^{γ_n} have a cut along the real axis line segment $-1 \leqslant \cosh \gamma_{0,n} \leqslant 1$ which in the z plane transforms into the whole of the circles (17) exactly. In our calculations we have selected a particular pair of branches; alternative choices would produce either the interior arcs themselves or combinations of these and the boundaries shown here. A similar problem of branch selection arises even in the original finite-size scaling calculations of Nightingale (1976) for real temperatures where γ_0 crosses the branch point at $e^{\gamma_0} = 1$.

Acknowledgments

One of us (RWT) wishes to thank the SERC for the award of a maintenance grant.

References

Barber M N 1983 *Phase Transitions and Critical Phenomena* vol 8, ed C Domb and J Lebowitz (Academic: New York) pp 145-266
Baxter R J, Enting I G and Tsang S K 1980 *J. Stat. Phys.* **22** 465
Bruscamp H J and Kunz H 1974 *J. Math. Phys.* **15** 65
Burkhardt T W and van Leeuven J M J 1982 *Real Space Renormalisation* vol 30 (Berlin: Springer)
Derrida B, De Seze L and Itzykson C 1983 *J. Stat. Phys.* **33** 559
Derrida B and Flyvbjerg H 1985 *J. Phys. A: Math. Gen.* **18** L313
Fisher M E 1965 *Lectures in Theoretical Physics* vol 7c (Boulder: University of Colorado Press) p 1
Itzykson C and Luck J M 1983 *Critical Phenomena and Theoretical Aspects*
Martin P P 1983 *Nucl. Phys* B. **225** 497
Nelson D R and Fisher M E 1975 *Ann. Phys., NY* **91** 226
Nightingale M P 1976 *Physica* **83A** 561
—— 1982 *J. Appl. Phys.* **53** 7927
Ono Y, Karaki M, Suzuki M and Kawabata C 1967 *Phys. Lett.* **24A** 703
—— 1968 *J. Phys. Soc. Japan* **25** 54
Onsager L 1944 *Phys. Rev.* **65** 117
Osbaldestin A H, Wood D W and Turnbull R W 1985 *J. Phys. A: Math. Gen.* **18** 1745
Pearson R B 1982 *Phys. Rev.* B **26** 6285
Wood D W 1985a *J. Phys. A: Math. Gen.* **18** L481
—— 1985b *J. Phys. A: Math. Gen.* **18** L917
Wood D W and Goldfinch M 1980 *J. Phys. A: Math. Gen.* **13** 2781

Wood D W and Osbaldestin A H 1982 *J. Phys. A: Math. Gen.* **15** 3579
—— 1983 *J. Phys. A: Math. Gen.* **16** 1019
Yang C N and Lee T D 1952a *Phys. Rev.* **87** 404
—— 1952b *Phys. Rev.* **87** 410